Effect of Zr addition on the fatigue strength of Cu-6Ni-2Mn-2Sn-2Al alloy

M. Goto[1], S.-Z. Han[2], C.-J. Kim[2] & N. Kawagoishi[3]
[1]Department of Mechanical Engineering, Oita University, Japan
[2]Korea Institute of Machinery & Materials, Korea
[3]Department of Mechanical Engineering, Kagoshima University, Japan

Abstract

Fatigue tests of Cu-6Ni-2Mn-2Sn-2Al alloy smooth specimens were carried out to clarify the effect of trace Zr on the fatigue strength. The growth behaviour of a major crack, which led to the final fracture of the specimen, was monitored to study the physical basis of fatigue damage. When stress amplitude was less than $\sigma_a = 350$ MPa, the fatigue life of Zr-containing alloys was about two times larger than that of alloys without Zr. When $\sigma_a > 350$ MPa, increments of fatigue life due to Zr decrease with an increase in σ_a and the increments were negligible at $\sigma_a = 400$ MPa. Increased fatigue life due to Zr addition resulted from an increase in crack initiation life and microcrack growth life. The growth rate of a small crack was determined by a term, $\sigma_a^n l$, independent of Zr addition. The effects of trace Zr on fatigue strength were discussed with relation to the initiation and propagation behaviour of a major crack.
Keywords: fatigue strength, small crack, crack growth rate, plastic replication technique, Cu-Ni-Sn alloy systems.

1   Introduction

The substitutes for Cu-Be alloys with a high production cost have been developed. Cu-Ni-Sn alloy systems have been regarded as potential substitutes for Cu-Be alloys. Among the Cu-Ni-Sn alloy systems, Cu-9Ni-6Sn alloys [1–4] are considered to have the best strength/ductility combination. When hot rolling is applied to produce sheet products, hot cracking problems occur [5] as a result of Sn-rich segregates formed during the solidification in castings. Cu-6Ni-2Mn-

2Sn-2Al alloys with a lower production cost and improved hot workability [6] have been recently developed as possible substitutes for Cu-9Ni-6Sn alloys. Mn is isomorphous compared to Cu and can partially replace the high-cost Ni which is beneficial to castability and tensile strength. The low Sn content makes it possible to be hot-rolled to produce sheet products. The addition of Al, which is a strong solid solution strengthener in Cu, gives this alloy a proper tensile strength without sacrificing the tensile ductility. The normal cast process for alloy production gives low production cost. Thus, Cu-6Ni-2Mn-2Sn-2Al alloys are applicable for various components in the electrical industry. However, further increase in the strength of alloys is required. It is known that the strength of pure copper is improved by the addition of a small amount of Zr, e.g., the precipitation hardening due to aging tends to saturate with the addition of only 0.15 % Zr. This indicates that the effects of small amounts of Zr addition to Cu-6Ni-2Mn- 2Sn-2Al alloys on the strength should be studied. On the other hand, when alloys are used for their actual components, it is important to estimate the fatigue damage of the material. To estimate fatigue damage precisely, the physical basis of fatigue damage must be clarified. However, there are only a few studies on fatigue of Cu-6Ni-2Mn-2Al alloys [7].

In the present study, fatigue tests of Cu-6Ni-2Mn-2Al alloys without and with Zr (0.1 and 0.3 %) have been carried out. The physical basis of fatigue damage and the effects of Zr addition on fatigue strength were discussed based on the initiation and growth behaviour of a crack monitored by the plastic replication technique.
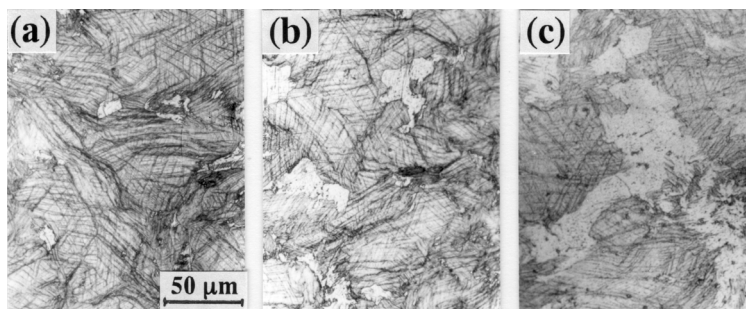

Figure 1:   Microstructure of the materials; (a) NZ, (b) Z1 and (c) Z3.

2   Experimental procedures

Cu-6Ni-2Mn-2Sn-2Al alloys without and with Zr (0.1 and 0.3 %) were prepared using a vertical continuous casting of high purity elemental Cu, Ni, Mn, Sn, Al and Zr in air. After casting, solution treatment was conducted at 850 $^{\circ}$C for 1 h, followed by swaging with a total swaging amount of 80 %. The diameter of swaged bars was 11 mm. Prior to machining the specimens, materials were aged at 400 $^{\circ}$C for 3 h. From here on, alloys without Zr, alloys with 0.1 and 0.3 % Zr are referred to NZ, Z1 and Z3, respectively. Fig.1 shows the microstructure of

the materials. Mechanical properties after aging were 876, 915 and 902 MPa tensile strength, 6.0, 7.0 and 6.3 % elongation, and 275, 288 and 287 Vickers hardness (load: 9.81 N) for NZ, Z1 and Z3, respectively.

Fig. 2 shows the shape and dimensions of the specimen. The round bar specimens with 5 mm diameter were machined from the bars. Although the specimens have a shallow circumferential notch (depth: $t = 0.25$ mm, radius: $\rho = 20$ mm), the strength reduction factor for this geometry is close to unity, so that the specimens can be considered as plain specimens. Before testing, all specimens were electro-polished to remove about 20 µm from the surface layer, in order to facilitate changes in the surface state.

All tests were carried out using a rotating bending fatigue machine with a constant bending moment type of a capacity of 14.7 Nm operating at 50 Hz. Specimens were fatigued at ambient air under constant stress amplitudes.

The observation of surface fatigue damage and the measurements of crack length were made via plastic replicas using an optical microscope at a magnification of x 400. The stress value used in the present study is that of the nominal stress amplitude, σ_a, at the minimal cross section. The crack length, l, is the length along the circumferential direction on the surface.
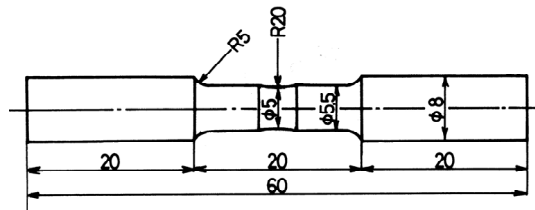

Figure 2:   Shape of the specimen.

3   Experimental results and discussion

3.1 Mechanical properties and S-N curve

Fig. 3 shows the S-N curve. The S-N curve of the Zr-containing alloys shifted toward the long life field, and showed a change in slope at around $\sigma_a = 350$ MPa. Namely, when stress amplitude is less than $\sigma_a = 350$ MPa, fatigue life of Zr-containing alloys is about 2 times larger than without Zr. When $\sigma_a > 350$ MPa, differences in fatigue life between alloys with and without Zr decrease with an increase in stress amplitude, and no increase in fatigue life at $\sigma_a = 400$ MPa is observed. In addition, the value of fatigue limit stress at 10^7 cycles, σ_w, was about 5 % larger in alloys with Zr than in alloys without Zr. With regard to the differences in Zr content between Z1 and Z3, Zr effects on fatigue strength were negligibly small.
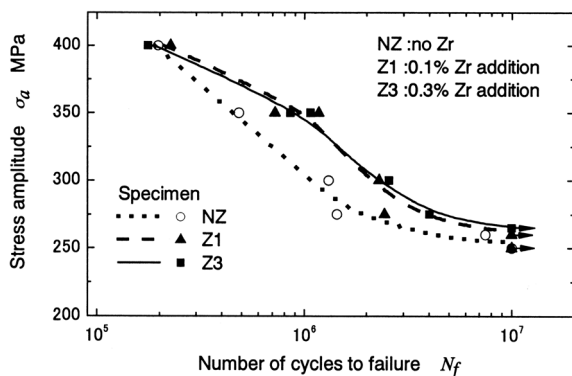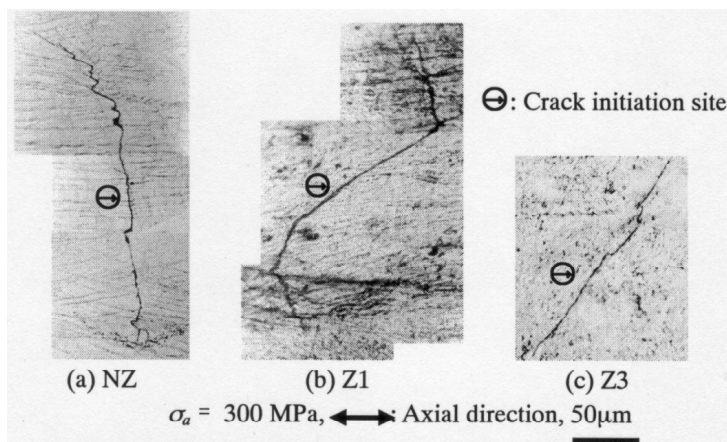
Figure 3:   S-N curve.

Figure 4:   Typical growth paths of a major crack.

3.2 Crack initiation and growth behaviour

Fig. 4 illustrates the typical growth paths of a major crack, which led to the final fracture of the specimen. The initiation site of a major crack was studied from the direct observation of surface etched after the detection of a 0.2mm length crack [7]. The results showed that, at σ_a = 300 and 350 MPa, the crack initiation site of NZ was grain boundaries (GBs), whereas the sites of Z1 and Z3 were the slip bands inside the grains. At σ_a = 400 MPa, both the GBs and slip bands were the initiation site of major cracks independent of the existence of Zr. With regard to other small cracks initiated after the major crack initiation, the initiation sites of those cracks were both the GBs and slip bands independent of stress amplitude and Zr addition.

Crack growth behaviour was monitored successively by the plastic replication technique, showing that, after initiation of a crack from GBs in NZ alloy, although the crack propagated along the initiation direction for a small

distance, it changed growth direction and propagated with a shear mode along the slip orientation within the adjacent grains. In Zr-containing alloys, a shear-mode crack from slip bands propagated along a slip orientation to GBs. A change in propagation direction occurred at GBs, followed by crack growth with shear-mode within the adjacent grains. In all alloys without and with Zr, when adjacent grains did not have suitable slip orientations for shear crack growth, crack growth with tensile mode was observed. Although growth behaviour of a small crack is influenced by the inhomogeneity of its microstructure, the influence of the microstructure on growth behaviour can be negligible for cracks larger than 0.3 mm. The propagation of relatively large cracks ($l > 0.3$ mm) was principally controlled by tensile mode. Similar growth behaviours have been observed in other cyclic-softening alloys such as age-hardened aluminium alloys [8–10]. As for the differences in Zr content, there were no significant differences in crack initiation and growth behaviour between the Z1 and Z3 alloys.

Fig. 5 shows the growth curve, the ln$l$ versus N relation, of a major crack. At $\sigma_a = 300$ and 350 MPa, the relation shifted toward the long life field due to the existence of Zr, but negligible effects of Zr addition on the growth curve were observed at $\sigma_a = 400$ MPa. Namely, at $\sigma_a = 400$ MPa, no significant differences in both the initiation life of a grain size order crack (e.g., $l \doteq 30$ μm) and the slope of crack growth curves were observed. Conversely, at $\sigma_a = 300$ and 350 MPa, addition of Zr increases the crack initiation life and makes the slope of the growth curves decrease. Strictly speaking, at $\sigma_a = 350$ MPa, crack growth behaviour in the range $l < 0.1$ mm is strongly retarded due to Zr addition. For $l > 0.1$ mm, although the slope of the growth curve for Zr-containing alloys tends to be slightly smaller than in alloys without Zr, its effect on growth life is practically negligible. Thus, Zr addition affects the behaviour of a crack propagating with low driving force (in other words, the smaller the crack length and stress amplitude, the larger the retardation of crack growth). Retardation of a
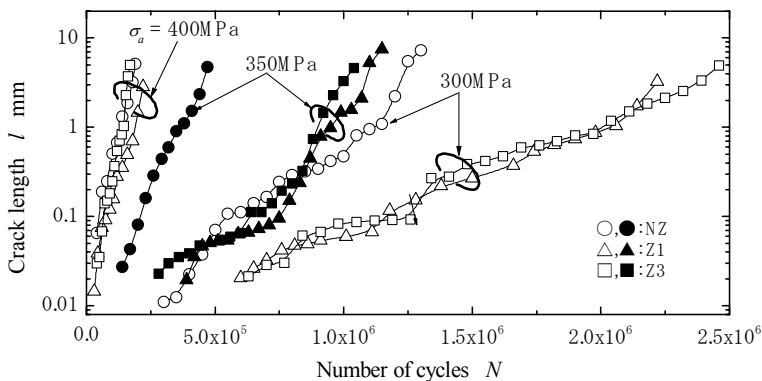

Figure 5: Crack growth curve (the ln$l$, logarithm of crack length, vs. N relation).

crack growth may be related to the strengthening of the matrix due to Zr addition. Since strengthening of the matrix is not relatively large (an increase in Vickers hardness was about 5 %), significant retardation of growth behaviour might occur for a small crack propagating under a low stress amplitude. On the other hand, the effects of difference in Zr content on crack initiation and crack growth behaviour are not clear.

Fig. 6 illustrates σ_a versus N_i and $N_{i \to f}$. N_i and $N_{i \to f}$ refer to the initiation life of a 0.05 mm crack and to the crack growth life from $l = 0.05$ mm to the fracture, respectively. When $\sigma_a \lesssim 350$ MPa, N_i for Z1 and Z3 is about 2 to 3 times larger than NZ. However, at $\sigma_a = 400$ MPa, a negligibly small increase in N_i due to Zr addition is observed. On the other hand, increments of $N_{i \to f}$ due to Zr addition gradually decrease with an increase in σ_a, and there is no difference in $N_{i \to f}$ at $\sigma_a = 400$ MPa. It has been shown in the previous report [7] that the significant large enhancement of crack initiation life in Zr-containing alloys was resulted from the strengthened GBs caused by the participation of Zr compounds.

In order to determine the compositions of Zr compounds precipitated at GB regions, energy-dispersive X-ray diffractometry (EDX) was used. However, accurate analysis failed because of the too small compound sizes. From the binary phase diagram, Zr never exists, taking the form of single particles in Cu-Ni-Mn-Sn-Al alloys because Zr tends to form compounds in Cu alloys. Table 1
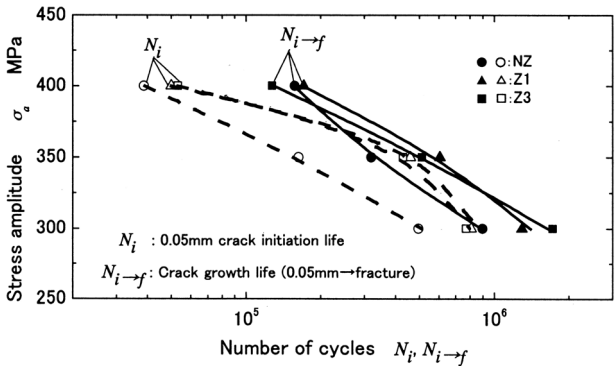

Figure 6:   Effects of Zr on crack initiation life, N_i, and crack growth life, $N_{i \to f}$.

Table 1:   Enthalpy of formation (ΔH_{for}) of the binary zirconium compounds.

Element	Compound	ΔH_{for}
Cu	$Cu_9 Zr_2$	-34
Ni	$Ni_3 Zr_2$	-73
Mn	$Mn_5 Zr_3$	-23
Sn	$SnZr$	-86
Al	$AlZr$	-83

ΔH_{for}: kJ/mole of atoms

shows the formation enthalpy of Zr-related compounds. SnZr and AlZr compounds show large formation enthalpy, while Al tends to solute in Cu matrix. Moreover, Sn tends to segregate at the GB regions when alloys were cast. Thus, we concluded that particles precipitated at GB regions are SnZr compounds.

3.3 Effect of Zr on the growth rate of a small crack

Fig.7 shows the *dl/dN* versus *l* relation of major cracks at σ_a = 300 MPa. Here, the crack growth rate *dl/dN* is calculated from the growth curve approximated by a smoothed curve. The range of crack length specified by "SMCG" indicates a crack propagating with shear mode. When the crack length was small (e.g., *l* < 0.2 mm), a crack tended to propagate with shear mode. For the crack length in excess of 0.2 mm, the propagation mechanism was principally dominant by tensile mode, and *dl/dN* is nearly proportional to *l*. Since a shear microcrack is strongly influenced by the inhomogeneity of its microstructure [11–15], the fluctuation of *dl/dN* is relatively larger than that of large crack propagating with tensile mode. In addition, the growth rate of SMCG is higher than that of a tensile-mode crack with corresponding crack length, evaluated from the relation holds for *l* > 0.3 mm.
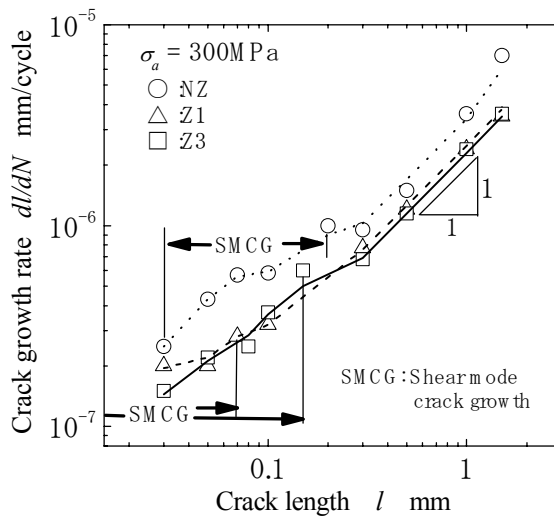

Figure 7:   *dl/dN* versus *l* relation (σ_a = 300 MPa).

The growth rate of fatigue crack was usually evaluated in terms of a stress intensity factor range *ΔK*. Here, *ΔK* is the effective parameter describing the stress field in the vicinity of a crack when the condition of small scale yielding at a crack tip is satisfied. The value of *ΔK* for an infinite plate with a through thickness crack is given by the equation $\Delta K = \Delta\sigma(\pi a)^{1/2}$. This equation indicates that the stress range has to be higher for a small crack in order to get the same

growth rate as for a large crack. However, when a sufficiently small crack propagates at finite growth rate (e.g., 10^{-6} - 10^{-3} mm/cycle), the condition of small scale yielding is not usually satisfied. Thus, the growth rate of a small surface crack cannot be determined uniquely by ΔK.

Nisitani and Goto [16–20] have studied small crack growth behaviour using carbon steels, low alloy steels, aluminium alloys, Ni-base superalloys and indicated that the growth rate of a small crack in which the condition of small scale yielding does not hold can be uniquely determined by a term $\sigma_a^n l$, but, not by the stress intensity factor range, i.e.

$$\frac{\mathrm{d}l}{\mathrm{d}N} = C_1 \sigma_a^n l \qquad (1)$$

In eqn (1), C_1 and n are material constants. Furthermore, they have proposed a convenient method for predicting the fatigue life based on the small crack growth law. The validity of the method has been confirmed by its application to the other researchers fatigue data [18]. The expression $\sigma_a^n l$ ($n = 3$) was first proposed by Frost and Dugdale [21]. They applied it to comparatively large cracks in which the condition of small scale yielding nearly holds. $\sigma_a^3 l$ can be considered as an application for ΔK, whereas $\sigma_a^n l$ in the present study is a parameter for crack propagating under large scale yielding.

Fig. 7 suggested that the dl/dN is proportional to l for a crack larger than $l = 0.3$ mm under the constant stress amplitude. The dependency of dl/dN on stress amplitude was also investigated and it was found that the dl/dN was proportional to σ_a^n for a constant crack length. The value of n for the present alloys was 8.0 independent of Zr addition. Putting these results together, we obtained the small crack growth law, eqn (1) with $n = 8$. Fig. 8 shows the dl/dN vs. $\sigma_a^8 l$ relation. The growth rate of a small crack ($l > 0.3$ mm) can be uniquely determined by eqn (1). With regard to the effect of Zr, trace Zr makes the growth rate slightly decrease.
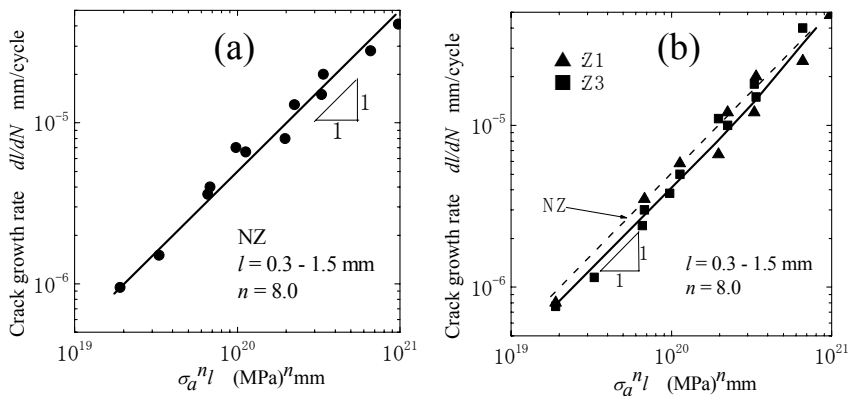

Figure 8: Crack growth data (dl/dN vs. $\sigma_a^n l$ relation); (a) relation for NZ alloy, (b) relation for Zr-containing alloys and comparison of the relation between non-Zr and Zr-containing alloys.

4   Conclusions

In order to study the fatigue behaviour of Cu-6Ni-2Mn-2Sn-2Al alloys without Zr, or with 0.1 and 0.3 % Zr, rotating bending fatigue tests of smooth specimens have been carried out. The plastic replication technique was used for monitoring crack initiation and growth behaviour. Here, alloys with no Zr, or containing 0.1 % Zr and 0.3% Zr were identified by the terms NZ, Z1 and Z3, respectively. The main conclusions can be summarized as follows:

(1) When the stress amplitude is less than $\sigma_a = 350$ MPa, fatigue life of Z1 and Z3 is about 2 to 2.5 times larger than that of NZ. When $\sigma_a > 350$ MPa, increments of fatigue life due to Zr addition decrease with an increase in σ_a and the increments are negligible at $\sigma_a = 400$ MPa. Thus, the S-N curve for Z1 and Z3 alloys shows a change in slope at around $\sigma_a = 350$ MPa. The increase in fatigue life in the range of $\sigma_a \lesssim 350$ MPa results from increases in crack initiation life and micro-crack growth life. With regard to differences in Zr content between Z1 and Z3, their effects on fatigue strength are negligibly small.

(2) The preferential initiation sites of a major crack, which led to the final fracture of specimens, in the range of $\sigma_a \lesssim 350$ MPa are grain boundaries (GBs) and slip bands for alloys with and without Zr, respectively. At $\sigma_a = 400$ MPa, both GBs and slip bands are initiation sites of the major cracks independent of the existence of Zr.

(3) Zr addition generated strengthened GBs resulting from precipitation of SnZr compounds. Strengthened GBs contributed to the increase in crack initiation life.

(4) The increase in microcrack growth life is related to the strengthening of matrix due to Zr addition. However, since the strengthening of the matrix is not large (e.g., the increase in H_V is about 5 %), significant retardation of growth behaviour can occur for a small crack propagating under a low stress amplitude less than $\sigma_a = 350$ MPa.

(5) Growth rate of a small crack can be determined by a term $\sigma_a^n l$. n is a material constant. The value of n was about 8 independent of Zr addition.

Acknowledgement

References

[1]   Plewes, J.T., *Metal Trans.*, **6A**, pp. 537-544, 1975.
[2]   Lefevre, B.G., Dannessa, A.T., Kalish, D., *Metall. Trans.*, **9A**, pp. 577-586, 1978.
[3]   Ray, R.K. & Narayanan, S.C., *Metall. Trans.*, **13A**, pp. 565-570, 1982.
[4]   Sato, A., Katsuta, S. & Kato, M., *Acta Metall Trans.*, **13A**, pp. 633-640, 1988.

[5]   Han, S.Z., Kim, H.I, Lee, J.M. & Kim, C.J., *J. Kor. Inst. Machinery Mater.*, **37**, pp. 882-886, 1999.
[6]   Rhu, C.J., Kim, S.S., Han, S.Z, Jung, Y.C. & Kim, C.J, *Scripta Mater.*, **42** pp. 83-89, 2000.
[7]   Goto, M., Han, S.Z., Kim, C.J. & Kawagoishi, N., *Mater. Letters*, to be published, 2007.
[8]   Goto, M., Nisitani, H., Kawagoishi, N., Miyagawa, H. & Chujoh, N., *Trans. Jpn Soc. Mech. Eng.* (in Japanese), **A-59**, pp. 205-211, 1993.
[9]   Goto, M., Kawagoishi, N., *J. Soc. Mater. Sci. Jpn* (in Japanese), **45**, pp. 675-680, 1996.
[10]   Goto, M. & DuQuesnay, D.L., *SAE Technical Paper Series*, **No.970703**, Soc. Automotive Engng-USA, pp. 1-7, 1997.
[11]   Suh, C.M., Yuuki, R. & Kitagawa, H., *Fatigue Fract. Engng Mater. Struct.,* **8**, pp.193-203, 1985.
[12]   Ochi, Y., Ishii, A. & Sasaki, S.K., *Fatigue Fract. Engng Mater. Struct.,* **8**, pp. 327-339, 1985.
[13]   Goto, M., *Fatigue Fract. Engng Mater. Struct.*, **14**, pp. 833-845, 1991.
[14]   Goto, M., *Fatigue Fract. Engng Mater. Struct.*, **16**, pp. 795-809, 1993.
[15]   Goto, M., *Fatigue Fract. Engng Mater. Struct.*, **17**, pp. 635-649, 1994.
[16]   Nisitani, H. & Goto, M., *The Behaviour of Short Cracks*, **EGF 1**, eds. K.J. Miller & E.R. de los Rios, Mech. Eng. Publications, London. pp.461-478, 1987.
[17]   Goto, M. & Nisitani, H., *Trans. Jpn. Soc. Mech. Eng.* (in Japanese), **A-56**, pp.1938-1944, 1990.
[18]   Nisitani, H., Goto, M. & Kawagoishi, N., *Eng. Fract. Mech.*, **41**, pp. 499-513, 1992.
[19]   Goto, M., *Fatigue Fract. Engng Mater. Struct.*, **17**, pp. 171-185, 1994.
[20]   Goto, M. & Knowles, D.M., *Eng. Fract. Mech.*, **60**, pp. 1-18, 1998.
[21]   Frost, N.E. & Dugdale, D.S., *J. Mech. Phys. Solids*, **6**, pp. 92-110, 1958.